Evolution of single-particle strength in neutron-rich ^{71}Cu

P. Morfouace[1], S. Franchoo[1], K. Sieja[2], I. Matea[1], L. Nalpas[3], M. Niikura[1], A. M. Sánchez-Benítez[4], I. Stefan[1], M. Assié[1], F. Azaiez[1], D. Beaumel[1], S. Boissinot[3], C. Borcea[5], R. Borcea[5], G. Burgunder[6], L. Cáceres[6], N. De Séréville[1], Zs. Dombrádi[7], J. Elseviers[8], B. Fernández-Domínguez[9], A. Gillibert[3], S. Giron[1], S. Grévy[10], F. Hammache[1], O. Kamalou[6], V. Lapoux[3], L. Lefebvre[1], A. Lepailleur[6], C. Louchart[3], G. Marquinez-Duran[4], I. Martel[4], A. Matta[1], D. Mengoni[11], D.R. Napoli[12], F. Recchia[11], J-A. Scarpaci[1], D. Sohler[7], O. Sorlin[6], M. Stanoiu[5], C. Stodel[6], J-C. Thomas[6] and Zs. Vajta[7]

[1]*Institut de Physique Nucléaire et Université Paris-Sud, 91406 Orsay Cedex, France*

[2]*Université de Strasbourg, IPHC, 67037 Strasbourg, France*

[3]*CEA Saclay, IRFU/SPhN, 91191 Gif-sur-Yvette Cedex, France*

[4]*Universidad de Huelva, 21071 Huelva, Spain*

[5]*Institute of Atomic Physics, IFIN-HH, Bucharest-Măgurele, P.O. Box MG6, Romania*

[6]*Grand Accélérateur National d'Ions Lourds, 14076 Caen Cedex 5, France*

[7]*Institute for Nuclear Research, Hungarian Academy of Sciences, 4026 Debrecen, Hungary*

[8]*Instituut voor Kern- en Stralingsfysica, University of Leuven, 3001 Leuven, Belgium*

[9]*Universidade de Santiago de Compostela, 15754 Santiago de Compostela, Spain*

[10]*Centre d'Études Nucléaires de Bordeaux Gradignan, 33175 Gradignan, France*

[11]*Dipartimento di Fisica e Astronomia dell'Università and INFN, 35131 Padova, Italy*

[12]*INFN Laboratori Nazionali di Legnaro, 35020 Legnaro, Italy*

Abstract

The strength functions of the $\pi f_{5/2}$, $\pi p_{3/2}$ and $\pi f_{7/2}$ orbitals in neutron-rich ^{71}Cu were obtained in a ^{72}Zn(d,^{3}He)^{71}Cu proton pick-up reaction in inverse kinematics using a radioactive beam of ^{72}Zn at 38 MeV/u. A dedicated set-up was developed to overcome the experimental challenges posed by the low cross section of the reaction and the low energy of the outgoing ^{3}He particles. The excitation-energy spectrum was reconstructed and spectroscopic factors were obtained after analysis of the angular distributions with the finite-range Distorted-Wave Born Approximation (DWBA). The results show that unlike for the $\pi f_{5/2}$ orbital and contrary to earlier interpretation, the $\pi f_{7/2}$ single-particle strength distribution is not appreciably affected by the addition of neutrons beyond $N = 40$.

Keywords:

1. Introduction

With a long and fruitful history to its credit, the shell model still accounts for much of our understanding of nuclear structure at low excitation energy [1]. The bulk of the interaction within the nuclear many-body system is well represented by a mean field that gives rise to a shell structure characterized by the well-known magic numbers 8, 20, 28, 50... which originally defined either proton or neutron closed shells. These magic numbers, however, are not absolute and universal but are subject to evolution as one moves away from the valley of stability into the realm of exotic isotopes, where the numbers of protons and neutrons are out of their ordinary balance.

The fate of a presumed doubly magic nucleus like ^{78}Ni therefore carries much interest, as its closed-shell character comes under scrutiny. While the ^{78}Ni isotope was observed for the first time two decades ago [2], only its half-life is known so far [3], which was measured more precisely recently [4] and direct spectroscopic information is not yet available. In this article, we investigate the $Z = 28$ gap that corresponds to the energy splitting between the $\pi f_{7/2}$ orbital and the $\pi p_{3/2}$ or $\pi f_{5/2}$ orbital. This is the first shell gap that originates from the spin-orbit interaction and its evolution away from stability gives insight into the isospin dependence of the spin-orbit force. The neutron-rich copper isotopes with one proton outside a nickel core present an ideal opportunity to probe the movement of a single-proton orbit in the field of a closed-shell nucleus. Proceeding along the copper isotopic chain, while filling of the $\nu g_{9/2}$ orbital ($40 < N \leq 50$), one is able to explore the influence of the occupation of the neutron orbitals on the nuclear structure.

Of particular interest is the transition at $N = 40$. Because the first excited state in ^{68}Ni is located at a rather high energy

and shows a spin and parity of 0^+, the existence of a subshell gap at $N = 40$ was rapidly acknowledged [5]. Nevertheless the small experimental $B(E2; 0_1^+ \rightarrow 2_1^+)$ value [6] was argued not to be a strong evidence for a magic ^{68}Ni nucleus [7]. Much experimental work has been done since, revealing a third 0^+ state at 2511 keV [8] and readjusting the second 0^+ energy to 1604 keV [9], which is consistent with a more recent study [10]. This has in turn spurred new theoretical activity, leading to a richer interpretation that advances the coexistence of spherical and deformed shapes in ^{68}Ni [11, 12].

The first excited state of spin and parity $5/2^-$ is situated in a stable manner at an energy between 1 and 1.2 MeV in the ^{63,65,67,69}Cu isotopes. In the β-decay of ^{71}Ni, it was observed that it suddenly comes down to 534 keV in ^{71}Cu [13]. This distinctive feature coincides with the addition of neutrons beyond $N = 40$. Because of the large spectroscopic factor of $C^2S = 1.5$ deduced in the ^{70}Zn(d,^{3}He)^{69}Cu proton pick-up reaction [14], the level can be interpreted as mainly corresponding to the $\pi f_{5/2}$ single-particle state in ^{69}Cu. For the level at 1190 keV in ^{71}Cu, seen in the $E2$ cascade that deexcites a $19/2^-$ microsecond isomer, a $7/2^-$ assignment was made [15, 16]. Based on a lower limit for the $\log ft$ value of 5.9 in the β-decay of ^{71}Ni, the ground state of which is conjectured to consist of a $9/2^+$ configuration, and the similarity of the γ branching pattern between ^{69}Cu and ^{71}Cu, a spin and parity of $7/2^-$ was suggested for the level at 981 keV. This was corroborated by calculations within the particle-core coupling model (PCM) that linked the state to the $f_{7/2}^{-1}$ proton hole, onto which a 2p–1h quasiband would dwell in the same manner as for ^{69}Cu [17]. The Coulomb excitation of ^{71}Cu accordingly revealed a value of 10.7(12) Weisskopf units for the 1190-keV level, while the 981-keV state was not observed and suggested to be of single-particle nature [18]. Finally the lifetime of the 981-keV state was measured in a recent study, which corresponds to $B(E2) = 44(20)\ e^2\ \mathrm{fm}^4$ [19]. In this article, since the theoretical value of the $B(E2)$ is much higher compared to the experimental one the authors exclude a particle-hole character for this state. Nevertheless one has to obtain spectroscopic factor for this state to confirm it.

The ^{71}Cu nucleus is an essential test for shell-model calculations because of the sudden change in the energy of the $\pi f_{5/2}$ orbital. The position of its spin-orbit partner, the $\pi f_{7/2}$ orbital, is important to measure the energy gap of the $Z = 28$ shell closure. In the present work, we set off to extract the spectroscopic factors of the $7/2^-$, $3/2^-$ and $5/2^-$ levels with the aim of obtaining the strength function of the single-particle states. We chose to do so in the ^{72}Zn(d,^{3}He)^{71}Cu proton pick-up reaction, as it should selectively populate the hole states in ^{71}Cu. Several papers have questioned the interpretation of spectroscopic factors as observables of single-particle components in nuclear wavefunctions [20, 21]. Nevertheless, it was shown that within a coherent parametrization of potential parameters, spectroscopic factors provide self-consistent information and are good indicators of orbital structures [22, 23].

2. Experimental setup

The experiment took place at the Ganil laboratory in Caen, France. A radioactive beam of ^{72}Zn at 38 MeV/u and a rate of 1.5 10^5 particles per second was obtained from the fragmentation of a primary ^{76}Ge beam on a Be target of 733 μm thickness. The reaction products were selected with the Lise spectrometer, resulting in a beam purity of 55% with ^{74}Ga as main contaminant (30%). Thanks to their time-of-flight difference, one is able to separate ^{72}Zn from ^{74}Ga and get a relative purity of 90.6%. After passing through two Cats beam-tracking detectors [24], the beam impinged on a deuterated polypropylene target of 0.26 mg/cm^2.

The target was surrounded by four Must2 telescopes [25], covering forward angles from 8 to 50° in the laboratory. The energy range of ^{3}He reaction product was below 21 MeV for laboratory angles lower than 46°. Since they would have been stopped already in the first stage of Must2, a double-sided silicon strip detector (DSSSD) of 300 μm, four silicon strip detectors with nominal thickness of 20 μm were added in front of the Must2 array. From transmission measurements with an α-source it appeared that the actual non-uniformity of the thickness varies up to 25%. Only after a pixel-by-pixel mapping on a 1-mm^2 grid was carried out to correct for the variation in energy loss (ΔE), the necessary resolution for particle identification could be achieved. Two Must2 telescopes covering the angles from $\theta_{lab} = 69°$ to $\theta_{lab} = 90°$ were installed in order to measure the elastic scattering, check the normalization and validate the optical potential in the incoming channel. Downstream from the experiment an ionization chamber was installed for detecting the outgoing heavy particles. The electronic dead time was kept at 15% throughout the experiment.

3. Data analysis and results

3.1. Excitation-energy spectrum and angular distributions

The ^{3}He particles of interest were identified by combination of their time-of-flight, ΔE signal in the 20-μm strip detectors and E deposit in the Must2 DSSSD. For each selected event, the excitation energy was reconstructed by the missing-mass method. The spectrum was further purified by requiring the presence of a heavy recoil in the ionization chamber. After the subtraction of background stemming from reactions on the carbon nuclei in the target (obtained in a separate run with a carbon target and shown in blue in Fig. 1), five peaks with an average resolution of $\sigma = 290$ keV (680 keV in FWHM) could be distinguished in the spectrum, as can be seen in Fig. 1 (a). The remaining events at negative energy, observed with low statistics, can be understood as stemming from the 9.4% beam contamination of ^{74}Ga. When comparing Fig. 1 (a) and 1 (b) one sees that the condition on the ionization chamber indeed reduces the ^{74}Ga counts.

Because of the limited angular coverage of the ionization chamber, its efficiency for our case amounted to 43% and its inclusion in the analysis reduces the statistics. Once the peaks in the excitation-energy spectrum are identified, we therefore remove the condition on the ionization chamber. The resulting

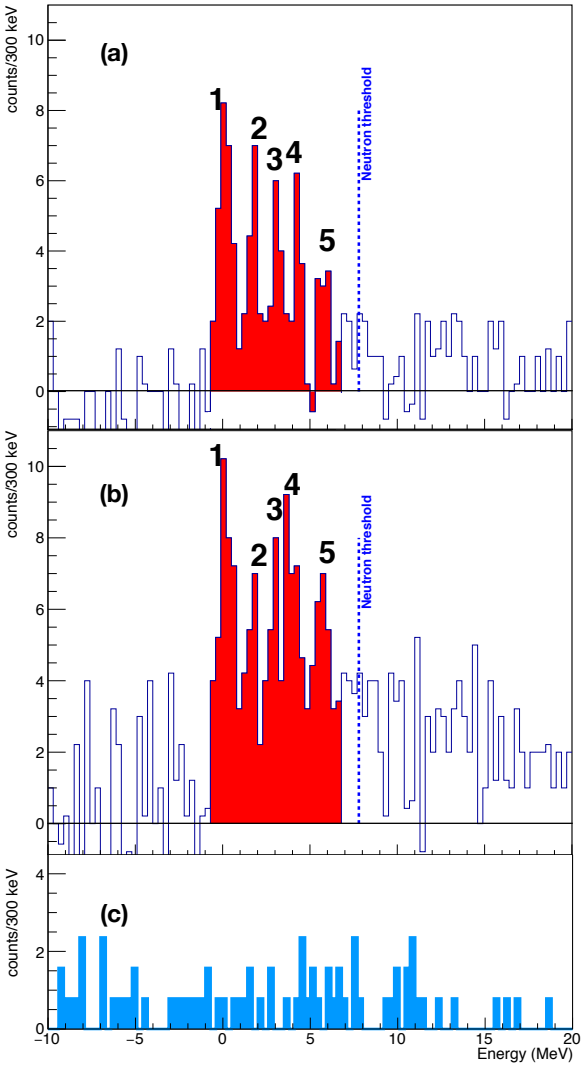

Figure 1: Excitation-energy spectrum of ^{71}Cu (a) with and (b) without condition on the ionization chamber. The red part corresponds to the identified states in ^{71}Cu. The blue dotted line shows the neutron threshold. The normalized carbon background (c) has been subtracted in the excitation-energy spectrum.

spectrum is shown in Fig. 1 (b). The width of the first peak is larger than the expected experimental resolution of σ = 306 keV (720 keV in FWHM) indicating the presence of a doublet. From the known level scheme [13, 18], the doublet can include two or more states among the $3/2^-$ ground state, the $1/2^-$ state at 454 keV and the $5/2^-$ state at 534 keV. For the latter a single-particle interpretation of $\pi f_{5/2}$ has been put forward and we should populate it in a similar manner as in ^{69}Cu [14]. The spectroscopic factor of the $1/2^-$ excited state in ^{69}Cu is three times weaker than for the $3/2^-$ ground state and its $B(E2)$ value is two times smaller than in ^{71}Cu, where it is known to be of a strongly collective nature [18]. We do not expect to see it in our pick-up reaction, therefore its possible contribution was not taken into account. The peak was fitted with a sum of two Gaussians, fixed at E_0 and E_0 + 0.534 MeV. The result is E_0 = 0.18(19) MeV and is consistent with zero within the statistical uncertainty. If the mean energy of the first peak is corrected for this offset, we find 0.11(19) MeV. In Tab. 1 we list the energies of the five identified peaks, corrected for the offset.

The angular distributions of the emitted ^{3}He particles were fitted with functions calculated within the finite-range Distorted-Wave Born Approximation (DWBA) using the DWUCK5 code. For the incoming channel, the relativistic Daehnick-F optical potential was taken [26] since it reproduces very well the angular distribution of the elastic scattering measured with the two Must2 detectors at 90°. For the outgoing channel, where the elastic scattering was not measured, we used the Perey and Perey parametrization [27]. The Pang potential [28] was also tested and a lower variation of 20% was observed for the spectroscopic factors. Nonetheless, after minimization, the χ^2 is worse since the shape of the calculated distribution using the Pang potential does not reproduce the experimental one as well as the Perey and Perey distribution does. For the overlap between the deuteron and the ^{3}He we chose the Brida potential [29]. Finally for the form factor the standard values of r_0=1.25 fm and a_0 = 0.65 fm were chosen. In our case, the use of different potentials affects the absolute normalization as expected but it does not affect the position of the energy distribution centroid.

After a χ^2 minimization, we found that the differential cross section of the first peak could be fitted with a combination of L = 1 and L = 3 distributions (Fig. 2 (a) assuming that it is a doublet, which is also consistent with the width of the peak. The L = 1 component shows a spectroscopic factor of C^2S = 0.8(2) (see Tab. 1), which we attribute to the $3/2^-$ ground state. The L = 3 contribution yields C^2S = 1.4(6) and we attribute it to the $5/2^-$ state at 534 keV, for which we infer a dominant $\pi f_{5/2}$ configuration. We note that the large spectroscopic factor exhausts the available $f_{5/2}$ proton strength as it was seen for the other lighter copper isotopes [14]. From the integrated cross sections of the L = 1 and L = 3 components taking into consideration their spectroscopic factors C^2S, we can determine the mean energy of the ground-state doublet. This gives 0.13 MeV, which agrees with the mean energy of the first peak of 0.11(19) MeV. The sum in the $\pi p_{3/2}$ and the $\pi f_{5/2}$ orbitals gives 2.2(6), which is compatible with the expected value of 2 protons in the zinc isotopes above Z = 28 and with former literature [14, 30].

The next three peaks were best fitted with L = 3 functions. The fourth peak is also wider and might contain at least two states but its angular distribution is well fitted with only L = 3. The weighted centroid for all the peaks gives 3.8 MeV. Since the shape of the L = 3 angular distribution does not change between 1.5 and 5 MeV excitation energy in the present reaction, the angular distribution of the three peaks together was fitted with a state at 3.8 MeV in the DWBA calculations. The result of the fit gives a spectroscopic strength of C^2S = 6.9(8) (Fig. 2 (b)), which is compatible with the sum of the respective spectroscopic factors ($\sum C^2S_{7/2^-}$ = 6.6(7)). This corresponds to 86±12% of the $\pi f_{7/2}$ strength with an experimental centroid at 3.8 MeV, which represents a lower limit as far as part of the strength stays undetected. One can see that the sum of the spectroscopic factors in the pf orbitals gives 9.1 ± 1.0, which is close to the expected value of 10 protons [31]. The fifth peak in

State	E (MeV)	$FWHM$ (MeV)	$L(J^\pi)$	C^2S
1	0.11(19)	0.95	1 $(3/2^-)$	0.8(2)
			3 $(5/2^-)$	1.4(6)
2	1.86(15)	0.61	3 $(7/2^-)$	1.4(2)
3	3.24(20)	0.61	3 $(7/2^-)$	1.5(3)
4	4.36(17)	0.94	3 $(7/2^-)$	3.7(6)
5	5.92(18)	0.94	0 $(1/2^+)$	0.4(1)
			2 $(3/2^+)$	3.0(5)

Table 1: Position in energy of the different populated states in ^{71}Cu with their width $FWHM$, the transferred angular momentum L, the proposed spin-parity J^π and the spectroscopic factor C^2S

E (MeV)	J^π	Percentage	Composition
0	$3/2^-$	60%	$\|0^+_\nu \otimes \pi p_{3/2}\rangle$
		14%	$\|2^+_\nu \otimes \pi p_{3/2}\rangle$
0.31	$5/2^-$	36%	$\|0^+_\nu \otimes \pi f_{5/2}\rangle$
		22%	$\|4^+_\nu \otimes \pi f_{5/2}\rangle$
1.09	$7/2^-$	47%	$\|2^+_\nu \otimes \pi p_{3/2}\rangle$
		11%	$\|4^+_\nu \otimes \pi p_{3/2}\rangle$
		10%	$\|J^+_\nu \otimes \pi f^{-1}_{7/2}\rangle$
1.41	$7/2^-$	42%	$\|2^+_\nu \otimes \pi f_{5/2}\rangle$
		12%	$\|4^+_\nu \otimes \pi f_{5/2}\rangle$
		13%	$\|J^+_\nu \otimes \pi f^{-1}_{7/2}\rangle$

Table 2: Dominating components of the wave functions for the lowest calculated states in ^{71}Cu

the excitation-energy spectrum was fitted with a superposition of $L = 0$ and $L = 2$ distributions even though in this case the χ^2 value is quite high ($\chi^2/NDF = 6.2/2$). One can infer that these states likely originate from hole excitations in the deeper *sd* shell.

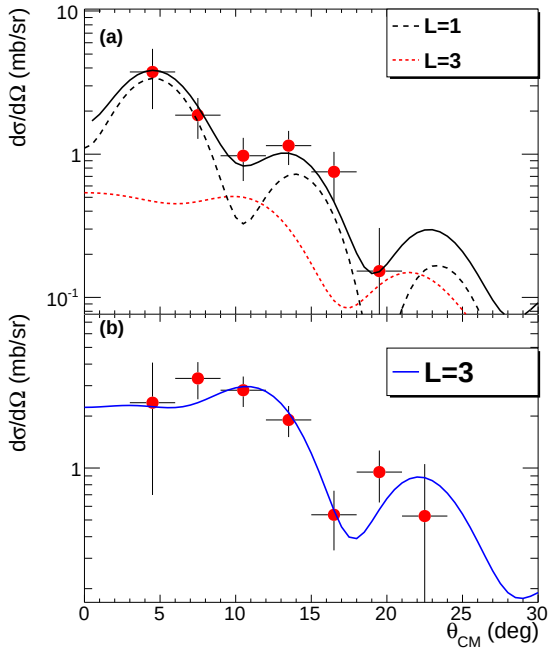

Figure 2: (a) Angular distribution of the first peak where a $L = 1$ and $L = 3$ angular distribution are needed. The black line corresponds to the minimization where both contributions are taken into account. (b) Summed angular distribution for the second, third and fourth peak in the excitation-energy spectrum of ^{71}Cu showing a $L = 3$ angular distribution.

3.2. Shell-model calculations

Shell-model calculations within a $fpgd$ valence space and originating from a Hamiltonian from earlier published work [32, 33] with minor modifications [19] were carried out. This valence space includes $\Delta l = 2$ valence orbitals for neutrons ($0g_{9/2}1d_{5/2}$) and protons ($0f_{7/2}1p_{3/2}$), which naturally favor quadrupole correlations and generate collectivity through the Elliott's $SU(3)$ symmetry [34]. One can see in Fig. 3 the comparison between the theoretical levels (C^2S_{th}) and the experimental ones (C^2S_{exp}). We can see in blue the strength function of the $\pi f_{5/2}$ levels. The experimental state situated at 534 keV is reproduced by the calculations at 310 keV. Concerning the strength function of the $f_{7/2}$ proton orbital, it appears more fragmented than the measurement could establish. Nevertheless, most of the distribution spreads around 2 and 4 MeV. The other smaller splinters remain below the experimental sensitivity. One can evaluate the evolution of the cumulative $\pi f_{7/2}$ strength by step of 2 MeV both experimentally and theoretically and note that the shapes of both curves are in fair agreement (cf Fig. 3 (c), giving confidence in the calculated trend even though the cumulative theoretical strength is larger than its experimental counterpart. This can be understood from the role of short and long-range correlations in the quenching of spectroscopic factors [35, 36].

In addition to the strength functions, calculations to determine the composition of the first low-lying states were performed (see Tab.2). We clearly see that the $3/2^-$ ground state mainly corresponds to a single proton in the $\pi p_{3/2}$ orbital. The $5/2^-$ is reasonably located and its dominant part corresponds to a single proton in the $\pi f_{5/2}$ orbital. It has to be noted that the energy gap between the effective single-particle energy (ESPE) from the shell-model calculations is decreasing between $\pi f_{5/2}$ and $\pi p_{3/2}$ due to the more attractive $\nu g_{9/2}-\pi f_{5/2}$ neutron-proton interaction. The high extracted spectroscopic factor combined with the calculations confirm the single-particle character of the $5/2^-$ state and the gradual weakening of the gap between the $\pi p_{3/2}$ and $\pi f_{5/2}$ orbitals.

We now come back to the nature of the two first $7/2^-$ states at 981 and 1190 keV respectively that are part of two γ cascades in ^{71}Cu. The one including the 1190-keV state shows an $E2$ sequence built on the $3/2^-$ ground state [15, 16]. The one including the 981-keV state forms a $\Delta L = 1$ pattern on top of the first $5/2^-$ level at 534 keV [37]. In our experiment, no pick-up strength was detected below 1.3 MeV except for the $L = 3$, $5/2^-$ state at 534 keV. Therefore, our data do not support the presence of a strong $L = 3$ component in the wave function of the $7/2^-$ state at 981 nor 1190 keV. As a matter of fact, the first calculated $7/2^-$ state at 1.09 MeV is dominated by the

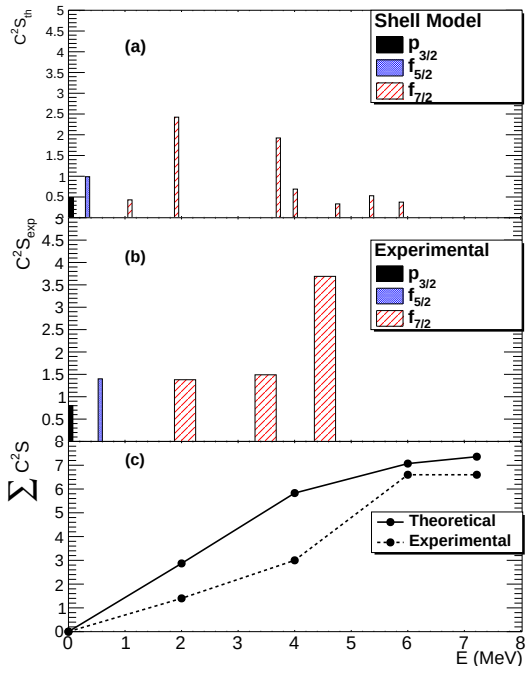

Figure 3: States from shell-model calculations with $C^2S_{th} > 0.3$ (a) compared to experimental data (b). The larger area for the experimental data stands for the experimental uncertainties for the $7/2^-$ states. Figure (c) corresponds to the accumulated strength both experimentally and theoretically.

coupling $|2^+_\nu \otimes \pi p_{3/2}\rangle$ and is associated with a strong calculated $B(E2)$ value to the ground state (179 e^2fm^4 or 10.25 W.u). It can be associated to the collective state at 1189 keV, which was observed in Coulomb excitation [18] with a measured value of $B(E2) = 10.7$ W.u. The wave function of the second calculated $7/2^-$ state has a large contribution coming from the coupling $|2^+_\nu \otimes \pi f_{5/2}\rangle$. It decays to the $5/2^-$ state and has a small calculated $B(E2)$ value (14.4 e^2fm^4 or 0.82 W.u) to the ground state. On the contrary, it has a strong calculated $B(M1)$ value to the $5/2^-$ state (0.168 μ_N^2). This state would correspond to the experimental level at 981 keV. We interpret the experimental results combined with the shell-model calculations as a dominant $M1$ character and it explains why this $7/2^-$ level at 981 keV was not seen in Coulomb excitation. Indeed it would involve a structurally different configuration, which would not be as favorable as the excitation to the $7/2^-$ level at 1190 keV. Taking together the preceding arguments, the non-observation of the level at 981 keV in our work excludes a $\pi f^{-1}_{7/2}$ interpretation of the level at 981 keV. The calculated spectroscopic factors of these two $7/2^-$ states are 0.43 and 0.007 respectively, which is below our experimental sensitivity and which can now be understood from the fact that these two states arise mainly from proton-core couplings. The $7/2^-$ states with a high spectroscopic factor are situated above 1.9 MeV both experimentally and theoretically. It indicates that the gap between $\pi f_{7/2}$ and $\pi p_{3/2}$ is not significantly reduced. The neutron-proton interaction is almost the same between $\nu g_{9/2} - \pi f_{7/2}$ and $\nu g_{9/2} - \pi p_{3/2}$ leading to the fact that the $Z = 28$ gap defined as the energy difference between the $\pi f_{7/2}$ and $\pi p_{3/2}$ ESPEs remains unchanged while the $\pi f_{5/2}$ orbital is getting closer to the $\pi p_{3/2}$ orbital.

From different experimental works [15, 16, 19, 37] and from this work, we see that three $7/2^-$ structures exist. In transfer we see that the $\pi f_{7/2}$ centroid does not come down therefore the $7/2^-$ levels at 981 and 1190 keV are not proton-hole states but from shell model calculations we identify them as $|2^+_\nu \otimes \pi f_{5/2}\rangle$ and $|2^+_\nu \otimes \pi p_{3/2}\rangle$ respectively. The last one was indeed seen in Coulomb excitation [18] while the first one was not observed because of its very low $B(E2)$ value. In this way, the results from β-decay, Coulomb excitation, deep-inelastic and transfer reaction are consistent with the present shell-model calculations.

The experimental data as well as the shell-model calculations show that the $f_{7/2}$ proton single-particle strength remains at several MeV of excitation energy in ^{71}Cu. It does not come down appreciably and does not follow the sharp decline of the $\pi f_{5/2}$ state, preventing a rapid reduction of the $Z = 28$ gap. It should be kept in mind, however, that the $\pi f_{7/2}$ orbital resides farther away from the Fermi surface and its influence on the nuclear structure at low energy is less immediate. Instead it appears more susceptible to fragmentation and therefore any change in its centroid is less visible than it is for its $\pi f_{5/2}$ spin-orbit partner. This is similar to observations of orbital energies in the $Z = 20$ region, where the experimental data [1, 38, 39] and the theoretical calculations [40] indicate a reduction of the $\pi d_{3/2} - \pi s_{1/2}$ gap in the potassium isotopes correlated with filling the $\nu f_{7/2}$ orbital, but the weakening of the gap between the $\pi d_{5/2} - \pi s_{1/2}$ orbitals is much less pronounced. From our findings, one can point to a parallel behavior in the copper isotopes where the $\pi f_{5/2} - \pi p_{3/2}$ gap is quenched with the filling of the $\nu g_{9/2}$ orbital, while we do not see any reduction of the $\pi f_{7/2} - \pi p_{3/2}$ gap.

4. Conclusion

Notwithstanding the low cross section of the order of 10 mb and the low energy of the outgoing light particles that did not exceed 7 MeV/u for the angles of interest leading to a challenging experimental setup, it has been possible for the first time to extract the spectroscopic factors for the (d,^{3}He) proton pick-up reaction with a ^{72}Zn radioactive beam in the neutron-rich copper region beyond $N = 40$. We confirm the weakening of the gap between the $\pi p_{3/2}$ and $\pi f_{5/2}$ orbitals and three levels carrying $\pi f_{7/2}$ strength were found in ^{71}Cu. Their spectroscopic factors were determined from the comparison of the experimental angular distributions with finite-range DWBA calculations. We found 86±12% of the $f_{7/2}$ proton strength and the centroid of the $\pi f_{7/2}$ force remains situated at several MeV of excitation energy contrary to earlier interpretation [17, 18], showing that there is no collapse of the $Z = 28$ shell gap in the neutron-rich copper isotopes.

The authors are thankful to the Ganil accelerator staff, informatics service and to the IPN design office. We are grateful for the grant of the Romanian National Authority for Scientific Research, CNCS - UEFISCDI, project number PN-II-ID-PCE-2011-3-048, to the grant FPA2010-22131-C02-01 from the Spanish government and to the OTKA contract No. K100835.

[1] O. Sorlin and M.-G. Porquet *Prog. in Part. and Nucl. Phys.* **61** 602 (2008).
[2] C. Engelmann *et al. Z. Phys.* A **352** 351(1995).
[3] P. Hosmer *et al. Phys. Rev. Lett.* **94** 112501 (2005).
[4] Z. Y. Xu *et al. Phys. Rev. Lett.* **113** 032505 (2014).
[5] M. Bernas, P. Dessagne, M. Langevin, J. Payet, F. Pougheon and P. Roussel *Phys. Lett.* B **113** 279 (1982).
[6] O. Sorlin *et al. Phys. Rev. Lett.* **88** 092501 (2002).
[7] K. Langanke *et al. Phys. Rev.* C **67** 044314 (2003).
[8] W. Mueller *et al. Phys. Rev.* C **61** 054308 (2000).
[9] F. Recchia *et al. Phys. Rev.* C **88** 041302 (2013).
[10] S. Suchyta *et al. Phys. Rev.* C **89** 021301(R) (2014).
[11] A. Dijon *et al. Phys. Rev.* C **85** 031301(R) (2012).
[12] Y. Tsunoda, T. Otsuka, N. Shimizu, M. Honma, Y. Utsuno *Phys. Rev.* C **89** 031301 (2014).
[13] S. Franchoo *et al. Phys. Rev. Lett.* **81** 3100 (1998).
[14] B. Zeidman and J.A. Nolen *Phys. Rev.* C **18** 2122 (1978).
[15] R. Grzywacz *et al. Phys. Rev. Lett.* **81** 766 (1998).
[16] T. Ishii *et al. Phys. Rev. Lett.* **81** 4100 (1998).
[17] A. Oros-Peusquens and P. Mantica *Nucl. Phys. A* **669** 81 (2000).
[18] I. Stefanescu *et al. Phys. Rev. Lett.* **100** 112502 (2008).
[19] E. Sahin *et al. Phys. Rev.* C **91** 034302 (2015).
[20] R. J. Furnstahl and H.-W. Hammer *Phys. Lett.* B **531** 203 (2002).
[21] T. Duguet and G. Hagen *Phys. Rev.* C **85** 034330 (2012).
[22] J. P. Schiffer *et al. Phys. Rev. Lett.* **108** 022501 (2012).
[23] J. P. Schiffer *et al. Phys. Rev.* C **87** 034306 (2013).
[24] S. Ottini *et al. Nucl. Instr. and Meth. in Phys. Res.* A **431** 476 (1999).
[25] E. Pollacco *et al. Eur. Phys. J.* A **25** 287 (2005).
[26] W.W. Daehnick, J.D. Childs and Z. Vrcelj *Phys. Rev.* C **21** 2253 (1980).
[27] C. Perey and F. Perey *At. Data and Nucl. Data Tabl.* **17** 1 (1976).
[28] D. Y. Pang *et al. Phys. Rev.* C **79** 024615 (2009).
[29] I. Brida, S.C. Pieper, R.B Wiringa *Phys. Rev.* C **84** 024319 (2011).
[30] G. Rotbard *et al. Phys. Rev.* C **18** 86 (1978).
[31] P. G. Hansen and J. A.Tostevin *Annu. Rev. Nucl. Part. Sci.* **53** 219 (2003).
[32] S.M. Lenzi, F. Nowacki, A. Poves and K. Sieja *Phys. Rev.* C **82** 054301 (2010).
[33] K. Sieja and F. Nowacki *Phys. Rev.* C **85** 051301(R) (2012).
[34] J.P. Elliott *et al. Proc. R. Soc. A.* **245** 128 (1958).
[35] W. H. Dickhoff and C. Barbieri *Prog. in Part. and Nucl. Phys.* **52** 377 (2004).
[36] C. Barbieri *Phys. Rev. Lett.* **103** 202502 (2009).
[37] G. De Angelis *Phys. Scr.* T **150** 014010 (2012).
[38] P. Doll *et al. Nucl. Phys. A.* **263** 210 (1976).
[39] S. M. Banks *et al. Nucl. Phys. A.* **437** 381 (1984).
[40] N. A. Smirnova *et al. Phys. Lett.* B **686** 109 (2010).